n-ZnO/p-GaN heterojunction light-emitting diodes featuring a buried polarization-induced tunneling junction

Ling Li, Yuantao Zhang, Long Yan, Junyan Jiang, Xu Han, Gaoqiang Deng, Chen Chi, and Junfeng Song

Citation: AIP Advances **6**, 125204 (2016); doi: 10.1063/1.4971272
View online: http://dx.doi.org/10.1063/1.4971272
View Table of Contents: http://aip.scitation.org/toc/adv/6/12
Published by the American Institute of Physics

n-ZnO/p-GaN heterojunction light-emitting diodes featuring a buried polarization-induced tunneling junction

Ling Li, Yuantao Zhang,[a] Long Yan, Junyan Jiang, Xu Han, Gaoqiang Deng, Chen Chi, and Junfeng Song
State Key Laboratory on Integrated Optoelectronics, College of Electronic Science and Engineering, Jilin University, Qianjin Street 2699, Changchun 130012, China

(Received 1 October 2016; accepted 15 November 2016; published online 5 December 2016)

n-ZnO/p-GaN heterojunction light-emitting diodes with a p-GaN/$Al_{0.1}Ga_{0.9}N$/n^+-GaN polarization-induced tunneling junction (PITJ) were fabricated by metal-organic chemical vapor deposition. An intense and sharp ultraviolet emission centered at ~396 nm was observed under forward bias. Compared with the n-ZnO/p-GaN reference diode without PITJ, the light intensity of the proposed diode is increased by ~1.4-folds due to the improved current spreading. More importantly, the studied diode operates continuously for eight hours with the decay of only ~3.5% under 20 mA, suggesting a remarkable operating stability. The results demonstrate the feasibility of using PITJ as hole injection layer for high-performance ZnO-based light-emitting devices. [http://dx.doi.org/10.1063/1.4971272]

ZnO has been considered as a promising material for ultraviolet (UV) light-emitting diodes (LEDs) and laser diodes owing to its high exciton binding energy of 60 meV and large direct band gap energy of 3.37 eV at room temperature.[1–3] At present, the reproducible fabrication of stable, high-quality p-type ZnO is still a challenge, which hinders the development of ZnO-based homojunction LEDs.[4–7] An alternative approach is to fabricate heterojunction devices by using other available p-type materials, such as p-GaN, p-Si, p-NiO, p-type organics etc.[8–15] Among them, GaN has been considered as the most suitable one because of its similar energy band structure and small lattice mismatch with ZnO. However, the staggered band alignment (type II) of the n-ZnO/p-GaN heterojunction inevitably causes an energy barrier at the heterointerface, resulting in low injected carriers that can cross the junction for electron-hole recombination and degrading the performance of the device. To solve this problem, one-dimensional ZnO nanorods (NRs) have been implemented to improve the carrier injection though nanosized heterojunctions.[16] Meanwhile, high homogeneous crystallinity presenting in ZnO NRs provides excellent transportation paths for injected electrons and serves as the escaping routes for trapped light to enhance the light extraction efficiency.[17] However, for all this, typical ZnO NRs/p-GaN LEDs still suffer from a low light output due to the inherently high resistivity of p-GaN layer. It is well known that the high resistivity may result in a poor current spreading within p-GaN layer, yielding inhomogeneous light emission. Furthermore, the junction heating effect at high current level also leads to failure of device operation, which seriously hinders the realization of commercial application for n-ZnO/p-GaN heterojunction LEDs. "Recently, making use of the strong spontaneous and piezoelectric polarization effects in III-nitrides, the polarization-induced tunneling junction (PITJ) has been widely investigated for both the metal-face (Ga/Al/In-face for c^+ growth orientation) and the nitrogen-face (N-face for c-growth orientation) III-nitride heterojunctions."[18–22] And employing PITJ as hole injection layer has been suggested as an efficient method to enhance the current spreading in GaN-based LEDs.[23–25] However, to date, PITJ has never been investigated or demonstrated for ZnO-based LEDs. In this work, n-ZnO NRs/p-GaN heterojunction

[a]Author to whom correspondence should be addressed. Electronic mail: zhangyt@jlu.edu.cn

LEDs with a p-GaN/$Al_{0.1}Ga_{0.9}N$/n^+-GaN PITJ were fabricated by metal-organic chemical vapor deposition (MOCVD). An enhanced light output and operating stability are simultaneously realized in the proposed diode owing to the improved current spreading and the subdued junction heating effect.

n-ZnO/p-GaN heterostructured LEDs with a p-GaN/$Al_{0.1}Ga_{0.9}N$/n^+-GaN PITJ were fabricated by two different MOCVD systems. First, p-GaN/$Al_{0.1}Ga_{0.9}N$/n^+-GaN PITJ was grown on commercially available *c*-plane Al_2O_3 substrates using AIXTRON CCS 3×2″ FT MOCVD. Trimethylaluminum (TMAl), trimethylgallium (TMGa) and high-purity ammonia (NH_3) were used as the source precursors for Al, Ga and N, respectively. Bis-cyclopentadienyl magnesium (Cp_2Mg) and silane (SiH_4) were employed as the p- and n-type GaN dopants, respectively. Hydrogen (H_2) was used as a carrier gas in the whole growth process. Prior to the deposition, Al_2O_3 substrate was cleaned in H_2 for 5 min at 1250 °C. After the growth of ~2 μm GaN template, a ~300 nm n-GaN layer was grown at 1040 °C, followed by a ~15 nm n^+-GaN layer with a Si doping concentration of $\sim 1 \times 10^{20}$ cm^{-3}. The temperature was then ramped up to 1060 °C for the growth of ~10 nm $Al_{0.1}Ga_{0.9}N$ layer, followed by a ~300 nm p-GaN layer with a Cp_2Mg doping concentration of $\sim 1 \times 10^{18}$ cm^{-3}. Thereafter, vertical-aligned ZnO NRs were prepared on the top of p-GaN films by photo-assisted MOCVD. Details on the growth of ZnO NRs can be found elsewhere.[26] For LEDs preparations, the standard lithography and etching steps were used. Au, In and Ni/Au were deposited on n-ZnO NRs, n-GaN and p-GaN films as contact electrodes, respectively. The surface morphology and crystallinity of ZnO NRs were investigated by field emission scanning electron microscopy (SEM; Jeol-7500F) and X-ray diffractometer (XRD; Rigaku Ultima IV), respectively. The photoluminescence (PL) spectra were recorded using a spectrometer (Jobin Yvon iHR550) with a He-Cd laser (325 nm, 20 mW) as the excitation source. The current-voltage (*I-V*) characteristics of the fabricated diode were measured by using a precision source/measure unit (Aligent B2902A). The electroluminescence (EL) measurement system used here consisted of a spectrometer (Zolix Omni-λ 500), and a photomultiplier.

Figure 1(a) shows the top-view SEM image of the prepared n-ZnO NRs arrays. The nearly vertical and homogeneous ZnO NRs with a diameter of ~100 nm can be clearly observed. Figure 1(b) presents the wide-range XRD pattern of the n-ZnO/p-GaN/PITJ heterostructure. The (0002) diffraction peaks of n-ZnO NRs, GaN and $Al_{0.1}Ga_{0.9}N$, and the (0006) diffraction peak of *c*-Al_2O_3 can be detected, indicating that the produced ZnO NRs arrays are preferentially oriented in *c*-axis direction. Figure 1(c) shows the PL spectrum of the produced n-ZnO NRs. The ZnO spectrum is characterized by a dominant UV emission peak located at 376 nm, which can be attributed to the near-band-edge (NBE) emission of ZnO. The absence of visible emission bands is the signature of very low concentration of defects in ZnO NRs, making the material suitable for use in UV LEDs.[27]

Fig. 2(a) shows the *I-V* characteristic of PITJ. The positive bias is defined when applying the positive voltage on the p-GaN layer. It can be seen that the reverse current is much higher than the forward current. At the same time, an obvious nonlinearity shows in the *I-V* curve at zero bias. These typical behaviors of backward-diode can be attributed to the interband tunneling effect in the AlGaN insert layer.[28,29] The interband tunneling can form the holes in the valence band of p-GaN. The good reverse bias characteristic indicates the big tunneling probability, which means that the produced

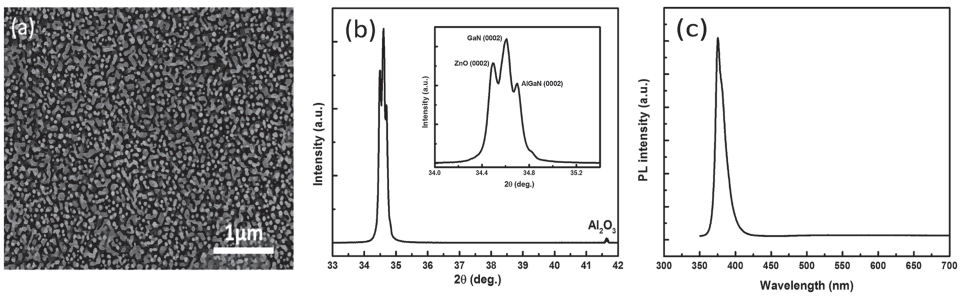

FIG. 1. (a) Top-view SEM image of ZnO NRs grown on p-GaN template. (b) XRD patterns of GaN, AlGaN and ZnO NRs. The inset of (b) shows the enlarged view of the (0002) peaks of ZnO NRs, p-GaN and $Al_{0.1}Ga_{0.9}N$. (c) PL spectrum of ZnO NRs.

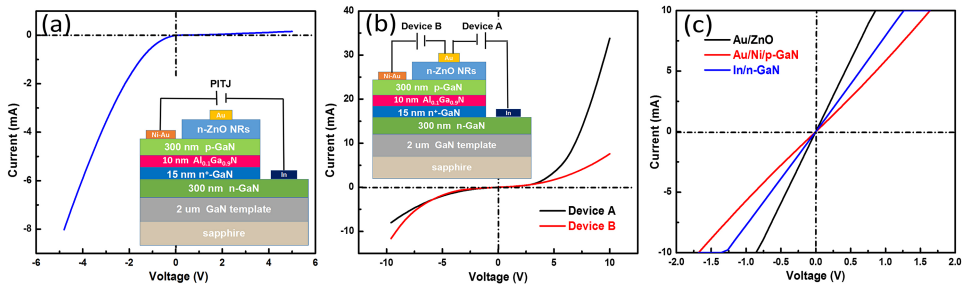

FIG. 2. (a) I-V characteristic of PITJ. The inset of (a) shows the schematic diagram of the PITJ device. (b) I-V characteristics of the device A and device B. The inset of (b) shows the schematic diagram of the three-terminal device. (c) I-V characteristics of Au on n-ZnO, Ni/Au on p-GaN and In on n-GaN.

PITJ can supply sufficient holes for the device. The inset of Fig. 2(b) shows the schematic diagram of the three-terminal device. When the voltage is applied across the n-GaN and the n-ZnO NRs, the device is an n-ZnO/p-GaN heterojunction with PITJ, marked as device A. When the voltage is applied across the p-GaN and the n-ZnO NRs, the device is a conventional n-ZnO/p-GaN heterojunction, marked as device B. Fig. 2(b) shows *I-V* characteristics of device A and device B. Both devices show clear rectification behavior with almost the same turn-on voltage of about 3 V. The measured series resistances of device A and device B are 253 Ω and 617 Ω at 7 mA, respectively. The decrease in series resistance of device A can be attributed to the reduction of lateral resistance and contact resistance by using n-GaN as the current spreading layer instead of p-GaN. The three linear curves, shown in the Fig. 2(c), reveal good Ohmic contacts of Au on ZnO, Au/Ni on p-GaN and In on n-GaN, which indicates the rectification behaviors arise from the heterojunctions.

Fig. 3(a) shows the EL spectra of device A ranging from 10 mA to 20 mA. A dominant UV emission at ~396 nm with a full width at half maximum of ~25 nm is observed, accompanied with a weak visible emission band at ~543 nm. As the current is increased, the EL emission peak position is almost unchanged and the corresponding intensity increases quickly. To understand the origins of the light emission of device A, a representative EL spectrum measured at 20 mA is decomposed with Gaussian functions. As shown in the inset of Figure 3(a), the strong emission peak centered at ~396 nm can be well composed of three different bands, which are NBE emission in n-ZnO around ~390 nm, donor-acceptor pair recombination in p-GaN around 422 nm, and radiative recombination at n-ZnO/p-GaN interface around 402 nm, respectively. The weak visible emission peak centered at ~543 nm comes from the defect-related deep level recombination in n-ZnO NRs. To verify the enhanced EL performance of the device A, the spectral characteristics of the referenced device B was measured for comparison. As shown in Figure 3(b), the EL performance of device B is similar to that of device A with a dominant UV emission at ~396 nm. Obviously, the device A could yield a more impactful emission output that that of device B. Fig. 3(c) shows the integrated EL intensities of device A and B as a function of driving currents. It can be seen that the EL intensities of device A

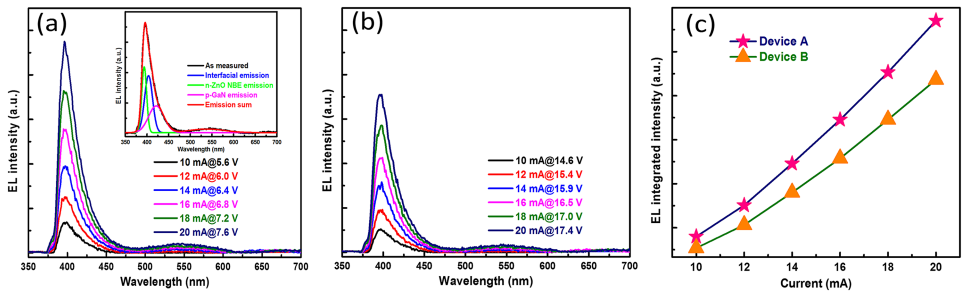

FIG. 3. (a) EL spectra of device A under different currents ranging from 10 mA to 20 mA. The inset of (a) shows the Gaussian decomposition of a representative EL spectrum from device A measured at 20 mA. (b) EL spectra of device B under different currents ranging from 10 mA to 20 mA. (c) Integrated EL intensities of device A and B as a function of driving currents.

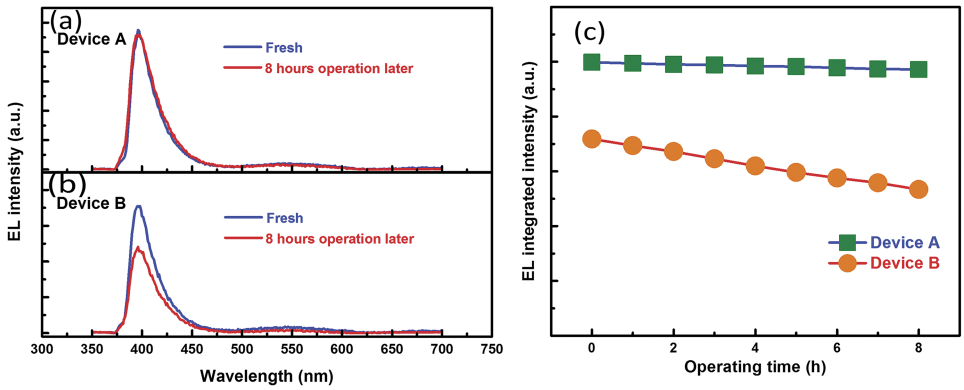

FIG. 4. (a) EL spectra of device A versus running time under a continuous current of 20 mA. (b) EL spectra of device B versus running time under a continuous current of 20 mA. (c) Integrated EL intensities of device A and device B as a function of operating time of the LED.

are higher than those of device B at all comparable currents. At the current value of 20 mA, the light output power of device A shows a ~1.4-folds enhancement compared to device B. The n-GaN layer in device A has a lower spreading resistance than p-GaN in device B, which increases the emission area in n-ZnO/p-GaN heterostructure diodes.[30] Therefore, we attribute the enhanced light output power of device A to the improved current spreading.

To estimate the suitability of the device A to practical LED applications, the preliminary stability study of the EL performance was carried out, in which a continuous current of 20 mA was injected and the light output power was intermittently recorded by using integrated EL intensity. As shown in Figure 4(a) and 4(b), the EL intensity of device B has a distinct decrease after 8 hours operation, while the intensity of device A almost remains the same. This suggests that the device A possesses a more excellent operating stability than device B. Furthermore, the integrated EL intensities of device A and device B as a function of operating time of the LED is plotted in Figure 4(c). For device A, the decrease trend is not obvious, and only ~3.5% decay in the light output power is observed after an operating time of 8 hours. The stability of the device A is greatly superior to the referenced device B where more than 32% decay is observed after aging under the same condition. We consider that the improved EL performance of device A can be attributed to the following aspects. Because the series resistance of device A is much lower than that of device B, the effect of junction heating in device A will be suppressed significantly compare to device B under the same driving current. As a result, device A can exhibit better operating stability than device B.

In conclusion, n-ZnO/p-GaN heterojunction LEDs with a p-GaN/$Al_{0.1}Ga_{0.9}N$/n^+-GaN PITJ were designed and fabricated. Compared with the n-ZnO/p-GaN heterojunction diode without PITJ, the proposed diode shows a higher light intensity and a remarkable operating stability. The improved performance of the studied diode can be attributed to the increased current spreading and the lower series resistance induced by the PITJ. The present work demonstrates that PITJ could be used as hole injection layer for high-performance ZnO-based LEDs.

This work was supported by the National Natural Science Foundation of China (Nos. 61274023, 61223005, 61376046 and 61674068), the National Key Research and Development Program (Nos. 2016YFB0400103), the Science and Technology Developing Project of Jilin Province (20150519004JH and 20160101309JC), and the Program for New Century Excellent Talents in University (NCET-13-0254).

[1] M. H. Huang, S. Mao, H. Feick, H. Yan, Y. Wu, H. Kind, E. Weber, R. Russo, and P. Yang, Science **292**, 1897 (2001).
[2] O. Lupan, T. Pauprté, and B. Viana, Adv. Mater. **22**, 3298 (2010).
[3] C. Bayram, F. H. Teherani, D. J. Rogers, and M. Razeghi, Appl. Phys. Lett. **93**, 081111 (2008).
[4] T. Y. Park, Y. S. Choi, and S. M. Kim, Appl. Phys. Lett. **98**, 251111 (2011).
[5] S. Li, Q. Wu, and G. Fan, Semicond. Sci. Technol. **24**, 085016 (2009).
[6] A. Allenic, W. Guo, and Y. B. Chen, Adv. Mater. **19**, 3333 (2007).
[7] H. S. Kang, G. H. Kim, and D. L. Kim, Appl. Phys. Lett. **89**, 181103 (2006).

[8] Ya. I. Alivov, J. E. Van Nostrand, D. C. Look, M. V. Chukichev, and B. M. Ataev, Appl. Phys. Lett. **83**, 2943 (2003).
[9] Q. X. Yu, B. Xu, Q. H. Wu, Y. Liao, G. Z. Wang, R. C. Fang, H. Y. Lee, and Ch. T. Lee, Appl. Phys. Lett. **83**, 4713 (2003).
[10] H. Sun, Q. F. Zhang, and J. L. Wu, Nanotechnology **17**, 2271 (2006).
[11] O. Lupan, T. Pauporté, and B. Viana, J. Phys. Chem. C **114**, 14781 (2010).
[12] Y. Y. Xi, Y. F. Hsu, A. B. Djurišić, A. M. C. Ng, W. K. Chan, H. L. Tam, and K. W. Cheah, Appl. Phys. Lett. **92**, 113505 (2008).
[13] B. Ling, J. L. Zhao, and X. W. Sun, Appl. Phys. Lett. **97**, 013101 (2010).
[14] B. M. Vermenichev, O. L. Lisitskiĭ, and M. E. Kumekov, Semiconductors **41**, 288 (2007).
[15] H. Ohta, M. Orita, and M. Hirano, J. Appl. Phys. **89**, 5720 (2001).
[16] S. K. Jha, C. Luan, C. H. To, O. Kutsay, J. Kovác, Jr., J. A. Zapien, I. Bello, and S. T. Lee, Appl. Phys. Lett. **101**, 211116 (2012).
[17] J. Ye, Y. Zhao, L. B. Tang, L. M. Chen, C. M. Luk, S. F. Yu, S. T. Lee, and S. P. Lau, Appl. Phys. Lett. **98**, 263101 (2011).
[18] S. Krishnamoorthy, D. N. Nath, F. Akyol, P. S. Park, M. Esposto, and S. Rajan, Appl. Phys. Lett. **97**, 203502 (2010).
[19] S. Krishnamoorthy, P. S. Park, and S. Rajan, Appl. Phys. Lett. **99**, 233504 (2011).
[20] S. Krishnamoorthy, F. Akyol, P. S. Park, and S. Rajan, Appl. Phys. Lett. **102**, 113503 (2013).
[21] K. X. Zhang, H. W. Liang, Y. Liu, R. S. Shen, W. P. Guo, D. S. Wang, X. C. Xia, P. C. Tao, C. Yang, Y. M. Luo, and G. T. Du, Sci. Rep. **4**, 6322 (2014).
[22] K. X. Zhang, H. W. Liang, R. S. Shen, D. S. Wang, P. C. Tao, Y. Liu, X. C. Xia, Y. M. Luo, and G. T. Du, Appl. Phys. Lett. **104**, 053507 (2014).
[23] Z. H. Zhang, S. T. Tan, Z. Kyaw, Y. Ji, W. Liu, Z. Ju, N. Hasanov, X. W. Sun, and H. V. Demir, Appl. Phys. Lett. **102**, 193508 (2013).
[24] S. Krishnamoorthy, F. Akyol, and S. Rajan, Appl. Phys. Lett. **105**, 141104 (2014).
[25] Y. Zhang, S. Krishnamoorthy, J. M. Johnson, F. Akyol, A. Allerman, M. W. Moseley, A. Armstrong, J. Hwang, and S. Rajan, Appl. Phys. Lett. **106**, 141103 (2015).
[26] H. G. Chen and Z. W. Li, Appl. Surf. Scie. **258**, 556 (2011).
[27] O. Lupan, T. Pauprtć, and B. Viana, Adv. Mater. **22**, 3298 (2010).
[28] S. Krishnamoorthy, D. N. Nath, F. Akyol, P. S. Park, M. Esposto, and S. Rajan, Appl. Phys. Lett. **97**, 203502 (2010).
[29] K. Zhang, H. Liang, Y. Liu, R. Shen, W. Guo, D. Wang, X. Xia, P. Tao, C. Yang, Y. Luo, and G. Du, Sci. Rep. **4**, 6322 (2014).
[30] S. R. Jeon, Y. H. Song, H. J. Jang, and G. M. Yang, App. Phys. Lett. **78**, 3265 (2001).